Partial-wave representations of laser beams for use in light-scattering calculations

Gérard Gouesbet, James A. Lock, and Gérard Gréhan

In the framework of generalized Lorenz–Mie theory, laser beams are described by sets of beam-shape coefficients. The modified localized approximation to evaluate these coefficients for a focused Gaussian beam is presented. A new description of Gaussian beams, called standard beams, is introduced. A comparison is made between the values of the beam-shape coefficients in the framework of the localized approximation and the beam-shape coefficients of standard beams. This comparison leads to new insights concerning the electromagnetic description of laser beams. The relevance of our discussion is enhanced by a demonstration that the localized approximation provides a very satisfactory description of top-hat beams as well.

1. Introduction

Many optical particle-sizing techniques rely on the interaction between laser beams and the particles that are being studied. Examples are provided by Gaussian laser beams used in phase-Doppler instruments,[1–3] laser sheets used in particle-image velocimetry,[4–6] and top-hat beams used in the so-called top-hat technique.[7–10] If the diameter of the spherical particles that are being studied is comparable to the characteristic beam width, the theoretical analysis of the light-scattering signature of the particles must rely on generalized Lorenz–Mie theory (GLMT) rather than on the usual plane-wave Lorenz–Mie theory.[11] A background in GLMT and its applications may be gained from Refs. 12–15.

In this formalism, shaped beams such as laser beams are mathematically expanded in terms of partial waves. The complex number that describes the amplitude and the phase of each partial wave in the expansion is called a beam-shape coefficient (BSC). These coefficients may be expressed as angular integrals of the radial component of the beam's electric and magnetic fields.[13] Unfortunately, none of the commonly used mathematical descriptions of laser beams is an exact solution of Maxwell's equations.[16–18] As a result, the BSC's produced by the angular integration of these fields retain a weak dependence on the radial coordinate,[19] in contrast with the fact that the derivation of the partial-wave decomposition demands that these coefficients be constants. The residual radial dependence is an artifact that results from the imperfect description of the electromagnetic fields of the beam.

On the other hand, a surprisingly accurate approximation to the BSC's is the so-called localized approximation.[20] It is a simple analytical expression whose accuracy is typically approximately 1 part in 10^5 from the value of the constant portion of the BSC's obtained by numerical integration.[21] This approximation relies on the localized interpretation of partial-wave expansions,[22] which is an analogy to van de Hulst's localization principle in Lorenz–Mie theory.[23] The localization approximation BSC's are constants as is required of partial-wave expansions, and the beam descriptions generated by insertion of these BSC's into the partial-wave expansion have been termed localized beams.[19] Such beams exactly satisfy Maxwell's equations because they are built from basis functions with constant coefficients.

Until recently, there had been no rigorous justification of the validity of the localized approximation. Initially, its validity was demonstrated by a comparison of the numerical values of the BSC's evaluated by the localized approximation with the values obtained by numerical integration or the finite series method.[21,24–26] When a beam propagates along the z axis of the coordinate system used to describe the

G. Gouesbet and G. Gréhan are with Laboratoire d'Energétique des Systèmes et Procédés, Unité de Recherche Associée Centre National de la Recherche Scientifique No. 230, Complex de Recherche Interdisciplinaire en Aérothermochemie, Institut National des Sciences Appliquées de Rouen, B.P. 08, 76131 Mont-Saint-Aignan, France. J. A. Lock is with the Department of Physics, Cleveland State University, Cleveland, Ohio 44115.

Received 27 June 1994.
0003-6935/95/122133-11$06.00/0.

partial-wave expansion, i.e., an on-axis beam, one of us recently succeeded in giving a derivation of the localized approximation[21] that relied on the stationary phase method, in analogy with van de Hulst's derivation of the localization principle.[23] The derivation, however, could not be generalized to off-axis beams, i.e., beams that are propagating parallel to but not along the z axis. By the use of another technique that relies on Taylor series expansions, a final derivation of the validity of the localized approximation for a focused Gaussian beam has been recently obtained for both the on-axis[19] and the off-axis cases.[27] This derivation uncovered a modification of the localized approximation that has been called the modified localized approximation.

A significant ingredient in the derivation was the discovery of the so-called standard-beam expressions. We strongly believe that standard beams will prove to be the best mathematical description of Gaussian beams. Standard beams exactly satisfy Maxwell's equations, because they are constructed from BSC's that are also constants. For the on-axis case, standard-beam BSC's are given by a simple infinite series[19] that results from an extrapolation of the Davis procedure[16] for description of the electromagnetic fields of a focused Gaussian beam. The standard-beam BSC's for the off-axis case have not yet been discovered, to our knowledge.

In this paper we consider two aspects of the partial-wave representation of laser beams for use in GLMT scattering calculations. (a) In the context of an on-axis focused Gaussian beam, we examine the convergence properties of the infinite series that describes the standard-beam BSC's. We also compare the values of the localized approximation and the modified localized approximation analytical expressions for the BSC's with the standard-beam BSC's that we use as a benchmark. We claim that the closer the localized approximation BSC's come to the standard-beam BSC's, the more accurate the localized approximation is in describing a focused Gaussian beam. (b) We apply the localized interpretation of partial-wave expansions to a top-hat beam and assess the accuracy of the resulting top-hat-beam localized approximation. To avoid burying the essence of the physics in complicated mathematical expressions, only the on-axis case is considered in this paper.

This paper is organized as follows. Section 2 summarizes the Davis formulation for description of the Gaussian beam electromagnetic fields and introduces the localized and the standard beams. Section 3 compares the numerical values of localized and standard-beam BSC's, providing new insights as to the nature of Gaussian beams and leading to the conclusion that standard beams should indeed be taken as the very definition of Gaussian beams. Section 4 further supports the validity of the localized interpretation of partial-wave analyses by describing the building of localized beams that provide a very satisfactory description of top-hat beams.

2. Davis, Standard, and Localized Descriptions of On-Axis Focused Gaussian Beams

A. Davis Formulation

A description of the electromagnetic fields of a focused Gaussian laser beam is provided by the Davis formulation.[16,17,28] We consider a Gaussian beam that is propagating along the z' axis from negative z' to positive z' (Fig. 1). Two parallel Cartesian coordinate systems must be used in this problem: (a) x', y', z', which is attached to the Gaussian beam and whose origin is at the center of the beam waist, and (b) x, y, z, which is used to describe the partial-wave expansion of the Gaussian beam. The origin of the $x'y'z'$ system with respect to the xyz system is z_0. We start by considering the simplest case, $z_0 = 0$, and below we examine the more general on-axis case with $z_0 \neq 0$ when appropriate.

We consider a monochromatic light wave with an $\exp(+i\omega t)$ time dependence. This time dependence will be omitted hereafter, as is the normal practice. In the Davis formulation a laser beam is described by a linearly polarized vector potential,

$$\mathbf{A} = (A_x, 0, 0). \tag{1}$$

The nonzero component A_x is given by

$$A_x = \psi(x, y, z)\exp(-ikz). \tag{2}$$

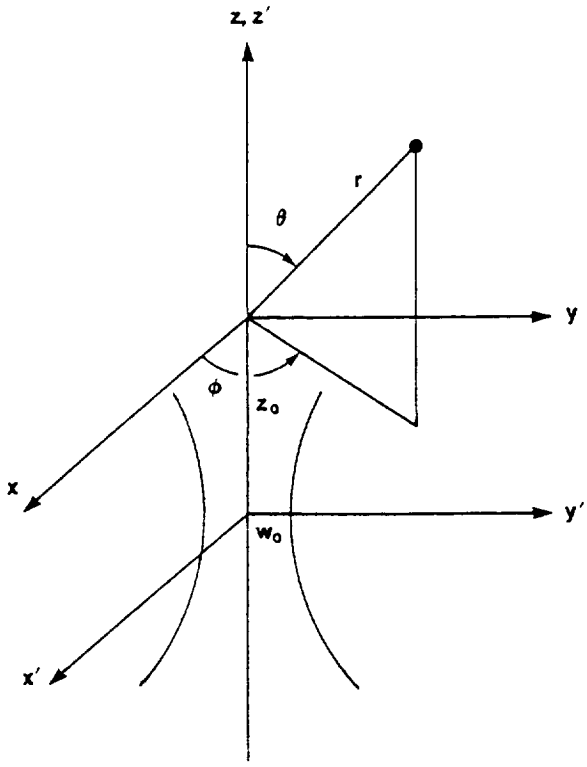

Fig. 1. Two coordinate systems that describe a focused Gaussian beam that is propagating along the z axis. The origin of the $x'y'z'$ coordinate system is at the center of the beam waist, and the partial-wave expansion is carried out with respect to the x, y, z coordinate system.

The function $\psi(x, y, z)$ is unknown and must be determined. Such a determination will involve spatial derivatives. However, the transverse coordinates x and y scale with a small transverse characteristic length w_0, and the coordinate z scales with a large longitudinal characteristic length l. The scaling lengths w_0 and l are taken to be the beam-waist radius and the spreading (or diffraction) length kw_0^2, respectively. Rescaled dimensionless coordinates (ξ, η, ζ) may therefore be introduced according to

$$\xi = \frac{x}{w_0}, \quad \eta = \frac{y}{w_0}, \quad \zeta = \frac{z}{l}. \tag{3}$$

The rescaled spatial derivatives $\partial\psi/\partial\xi$, $\partial\psi/\partial\eta$, and $\partial\psi/\partial\zeta$ are now of the same magnitude.

Within the Lorentz gauge, the vector potential $\mathbf{A}$ must satisfy the Helmholtz equation,

$$\nabla^2\mathbf{A} + k^2\mathbf{A} = 0, \tag{4}$$

providing the partial differential equation for ψ:

$$\left(\frac{\partial^2}{\partial\xi^2} + \frac{\partial^2}{\partial\eta^2}\right)\psi - 2i\frac{\partial\psi}{\partial\zeta} + s^2\frac{\partial^2\psi}{\partial\zeta^2} = 0. \tag{5}$$

In Eq. (5) we have introduced the small dimensionless parameter s given by

$$s = w_0/l = 1/kw_0. \tag{6}$$

Because s is the ratio of two characteristic length scales that define the overall aspect of the beam, we name it the beam-confinement factor. For a plane wave with $w_0 \to \infty$, the beam-confinement factor is zero. Even for commonly encountered Gaussian beams, this factor is usually very small. For instance, for $\lambda = 0.5$ μm and $w_0 = 50$ μm, we have $s \approx 10^{-3}$. There is, however, an upper theoretical limit to s that is discussed at the end of this subsection.

The function ψ is expanded in powers of s^2 as

$$\psi = \psi_0 + s^2\psi_2 + s^4\psi_4 + \ldots. \tag{7}$$

The lowest-order term ψ_0 represents the fundamental mode of the Gaussian beam. By the use of Eq. (5), it is easily checked that this mode is

$$\psi_0 = iQ\exp[-iQ(\xi^2 + \eta^2)], \tag{8}$$

$$Q = \frac{1}{i + 2\zeta}. \tag{9}$$

Once ψ_0 is known, Eq. (5) implies that the higher-order functions ψ_{2n} for $n \geq 1$, i.e., corrections to the fundamental mode, may be recursively deduced from

$$\left(\frac{\partial^2}{\partial\xi^2} + \frac{\partial^2}{\partial\eta^2} - 2i\frac{\partial}{\partial\zeta}\right)\psi_{2n-2} = -\frac{\partial^2}{\partial\zeta^2}\psi_{2n}, \quad n \geq 0. \tag{10}$$

The functions ψ_2 and ψ_4 are more complicated[16,17] than ψ_0. Because $\psi_2, \psi_4, \ldots$ depend on ψ_0 through Eq. (10), the fundamental mode ψ_0 alone completely determines the vector potential $\mathbf{A}$ from which electric and magnetic fields are derived by the use of

$$\mathbf{E} = \frac{-ic}{k}\nabla(\nabla\cdot\mathbf{A}) - i\omega\mathbf{A}, \tag{11}$$

$$\mathbf{H} = (\nabla\times\mathbf{A})/\mu, \tag{12}$$

leading to

$$E_x = E_0\left[\psi_0 + s^2\left(\psi_2 + \frac{\partial^2\psi_0}{\partial\xi^2}\right) + \ldots\right]\exp(-ikz), \tag{13}$$

$$E_y = E_0\left[s^2\frac{\partial^2\psi_0}{\partial\xi\partial\eta} + s^4\frac{\partial^2\psi_2}{\partial\xi\partial\eta} + \ldots\right]\exp(-ikz), \tag{14}$$

$$E_z = E_0\left[-is\frac{\partial\psi_0}{\partial\xi} - is^3\left(\frac{\partial\psi_2}{\partial\xi} + i\frac{\partial^2\psi_0}{\partial\xi\partial\zeta}\right) + \ldots\right]\exp(-ikz), \tag{15}$$

$$H_x = 0, \tag{16}$$

$$H_y = H_0\left[\psi_0 + s^2\left(\psi_2 + i\frac{\partial\psi_0}{\partial\zeta}\right) + \ldots\right]\exp(-ikz), \tag{17}$$

$$H_z = H_0\left[-is\frac{\partial\psi_0}{\partial\eta} - is^3\frac{\partial\psi_2}{\partial\eta} + \ldots\right]\exp(-ikz). \tag{18}$$

Assume that a Gaussian laser beam is focused to a radius w_0 equal to λ or even $\lambda/2$, corresponding to $s = 0.16$ and $s = 0.32$, respectively. The so-called diffraction or confinement limit dictates that the beam cannot be focused any more tightly than this. The existence of this limit may be understood in a qualitative and intuitive manner as follows. First consider a plane wave that is propagating in the positive z direction with its electric field polarized in the x direction. The variation of E_x in the z direction (i.e., one cycle of variation over the distance $\Delta z = \lambda$) induces a magnetic field H_y. Similarly, the variation of H_y in the z direction induces a new electric field E_x. Together the two fields E_x and H_y recursively induce each other, causing the forward propagation of the plane wave. Now consider a beam with a Gaussian profile in the x–y plane that is again propagating in the positive z direction. The additional variation of E_x in the y direction induces a new magnetic field H_z, and the additional variation of H_y in the x direction induces a new electric field E_z. The variations of E_z and H_z induce yet other fields. Together the new fields E_z and H_z cause the beam to spread transversely as it propagates. When E_x and H_y are slowly varying in the x–y plane (i.e., $w_0 \gg \lambda$ or $s \ll 1$), the induced fields E_z and H_z are weak and the spreading is slow. But when E_x and H_y are as rapidly varying in the x–y plane as they are in the z direction (i.e., $w_0 \approx \lambda$ or $s \approx 1/2\pi$), the induced fields E_z and H_z are strong, and the transverse spreading of the beam is as rapid as its forward propagation. The transverse spread-

ing resembles the nearly isotropic radiation from a point source more than it does a transversely localized beam that is propagating in a definite and unambiguous direction. Therefore the range $0.16 \leq s \leq 0.32$ indicates a range for the theoretical limit between the directional propagation of a beam and an isotropically radiating source. A similar limit occurs for Fraunhofer diffraction by an aperture of half-width a. For $2a > \lambda$, the diffraction pattern contains both relative maxima and relative minima, indicating direction dependence. But for $2a \ll \lambda$, the diffraction pattern is nearly isotropic in the forward hemisphere.

We may also introduce the kth Davis beam approximation defined when only those terms in Eqs. (13)–(18) that explicitly depend on s up to and including the power s^k are retained. We obtain the first Davis beam ($k = 1$) depending on ψ_0 and containing terms up to s^1; the third Davis beam ($k = 3$) depending on ψ_0, ψ_2, and containing terms up to s^3; the fifth Davis beam ($k = 5$) depending on ψ_0, ψ_2, ψ_4 and containing terms up to s^5; and so on.[19] None of these beams is an exact solution of Maxwell's equations. Maxwell's equations are only satisfied in the limit $k \to \infty$.

B. Standard Beams

In the framework of GLMT, an on-axis laser beam is described by the set of BSC's g_n given by[13]

$$g_n = -\frac{1}{2} i^{n-1} \frac{R}{j_n(R)} \frac{1}{n(n+1)} \int_0^{\pi} \sin^2\theta \, d\theta f(R, \theta) \times \exp(-iR\cos\theta) P_n^1(\cos\theta), \quad (19)$$

in which r, θ, ϕ are spherical coordinates (Fig. 1), $R = kr$, $j_n(R)$ are spherical Bessel functions, P_n^1 are associated Legendre polynomials, and $f(R, \theta)$ is defined by

$$\begin{pmatrix} E_r/E_0 \\ H_r/H_0 \end{pmatrix} = \exp(-iR\cos\theta) f(R, \theta) \sin\theta \begin{pmatrix} \cos\phi \\ \sin\phi \end{pmatrix}. \quad (20)$$

Consider the kth Davis beam approximation and denote its radial electric and magnetic fields by E_r^k and H_r^k, respectively, with $k = 1, 3, 5$ for the first, third, and fifth Davis beams, respectively. These lead to the first-order, third-order, and fifth-order approximations g_n^k to the BSC's in the following way.[19] The approximation f^k to f is Taylor series expanded in powers of the small parameter s, which permits an analytical integration of Eq. (19). When this is done, it is found that nonconstant terms occur; i.e., the result of the integral does not cancel the prefactor $R/j_n(R)$, contradicting the fact that the BSC's must be constants. The occurrence of such nonconstant terms is due to the fact that the approximations E_r^k and H_r^k do not exactly satisfy the Maxwell equations. However, the nonconstant terms appear at increasingly higher powers of s when k increases. For $k = 1$, the $O(s^0)$ and $O(s^2)$ terms are found to be constants, with nonconstant terms occurring at $O(s^4)$ and higher. For $k = 3$, nonconstant terms occur at $O(s^8)$ and higher, and they occur at $O(s^{12})$ and higher for $k = 5$. Because we understand that the nonconstant terms are artifacts produced by the approximate nature of the beam descriptions, they may be dismissed. Because the details of the computations require much algebra, it is somewhat of a pleasant surprise that the resulting g_n^ks for $k = 1, 3, 5$ may be written in the simple form,

$$g_n^k = \sum_{l=0}^{k} (-1)^l \frac{s^{2l}}{l!} \frac{(n-1)!}{(n-1-l)!} \frac{(n+1+l)!}{(n+1)!}, \quad (21)$$

which explicitly leads to

$$g_n^1 = 1 - (n-1)(n+2)s^2, \quad (22)$$

$$g_n^3 = g_n^1 + \tfrac{1}{2}(n-2)(n-1)(n+2)(n+3)s^4 - \tfrac{1}{6}(n-3)(n-2)(n-1)(n+2)(n+3) \times (n+4)s^6, \quad (23)$$

$$g_n^5 = g_n^3 + \tfrac{1}{24}(n-4)(n-3)(n-2)(n-1)(n+2) \times (n+3)(n+4)(n+5)s^8 - \tfrac{1}{120}(n-5)\ldots \times (n-1)(n+2)\ldots(n+6)s^{10}. \quad (24)$$

The same procedure may be carried out for the general on-axis case with $z_0 \neq 0$. The amount of algebra is, however, now so great that by-hand computations are unreasonable, and use of symbolic computation software such as MAPLE is compulsory. Still, the g_n^k's end up being given by the relatively simple expression[19]

$$g_n^k = \sum_{j=0}^{j+2l=k} \sum_{l=0}^{2k+1} \left(\frac{-2isz_0}{w_0}\right)^j (-1)^l s^{2l} \frac{(l+j)!}{l!\,j!} \frac{1}{l!} \times \frac{(n-1)!}{(n-1-l)!} \frac{(n+1+l)!}{(n+1)!} \exp(ikz_0). \quad (25)$$

Equation (25) represents the most general and rigorous result for the analytical evaluation of the BSC's, which we call the s-expansion method.

Although s is usually small, it is demonstrated in Subsection 2.C. that even g_n^5, which contains terms of up to $O(s^{10})$, is not sufficient to describe extremely focused beams or the BSC's accurately for large partial waves. Because the amount of algebra that would be required for higher-order Davis beams to be designed and the corresponding g_n^k's to be evaluated is extensive, it is appealing to conjecture that Eqs. (21) and (25) remain valid for $k > 5$. The infinite generalization then reads

$$g_n^\infty = \sum_{j=0}^{\infty} \sum_{l=0}^{\infty} \left(-2is\frac{z_0}{w_0}\right)^j (-1)^l s^{2l} \frac{(l+j)!}{l!\,j!} \frac{1}{l!} \times \frac{(n-1)!}{(n-1-l)!} \frac{(n+1+l)!}{(n+1)!} \exp(ikz_0), \quad (26)$$

which reduces to

$$g_n^{\,s} = \sum_{l=0}^{s} \frac{(-1)^l s^{2l}}{l!} \frac{(n-1)!}{(n-1-l)!} \frac{(n+1+l)!}{(n+1)!} \quad (27)$$

for $z_0 = 0$.

We call Eqs. (26) and (27) the standard BSC's, and the beam defined by this set of BSC's is called a standard beam. The $g_n^{\,k}$ coefficients of Eqs. (21) and (25) will be called the kth-order approximation to the standard BSC's. We claim that standard beams should be taken as the ideal description of Gaussian beams. This claim will be reinforced by the numerical results of Section 3. But before proceeding to these numerical results, we must introduce the localized approximation to the BSC's of Eq. (19).

C. Localized Approximation

The localized approximation for a focused Gaussian beam[20] is built on the first-order Davis beam of Eqs. (8) and (9) and results from the localized interpretation of partial-wave expansions. For $z_0 = 0$, the radial electric field of the first-order Davis beam in Eq. (11) may be written as

$$E_r = E_0 \exp(-ikz)\sin\theta \cos\phi f(kr, \theta), \quad (28)$$

with

$$f(kr, \theta) = iQ \exp\left(-iQ \frac{r^2 \sin^2\theta}{w_0^2}\right)(1 - 2Qsr \cos\theta / w_0). \quad (29)$$

The localized approximation $\bar{g}_n$ to the BSC's g_n is obtained by application of the localization operator $\hat{L}$ to the function f in Eq. (29) according to the prescription

$$\hat{L} f(R, \theta) = f(n + \tfrac{1}{2}, \pi/2), \quad (30)$$

which is the van de Hulst localization principle applied in the focal plane of the beam.[22] The integration in Eq. (19) may then be easily performed,[21] yielding

$$\overline{g_n} = \exp[-s^2(n + \tfrac{1}{2})^2]. \quad (31)$$

To motivate the modified localized approximation, we now demonstrate that the standard BSC's $g_n^{\,s}$ of Eq. (27) may be approximated by

$$g_n^{\,s} \approx \exp[-s^2(n-1)(n+2)]. \quad (32)$$

The demonstration proceeds in the following way. The exponential in Eq. (32) may be expanded as

$$\exp[-s^2(n-1)(n+2)] = g_n^{\,1} + \tfrac{1}{2}\alpha(n-2)(n-1)(n+2)(n+3)s^4 - \tfrac{1}{6}\beta(n-3)(n-2)(n-1)(n-2)(n+3) \times (n+4)s^6 + \ldots, \quad (33)$$

where $g_n^{\,1}$ is given by Eq. (22) and

$$\alpha = \frac{(n-1)(n+2)}{(n-2)(n+3)}, \quad (34)$$

$$\beta = \frac{(n-1)^2(n+2)^2}{(n-3)(n-2)(n+3)(n+4)}. \quad (35)$$

The behavior of α and β as a function of the partial wave n is illustrated in Table 1. For small partial waves, when α and β are significantly different from 1, the difference between the exponential in relation (32) expanded up to $O(s^6)$ and $g_n^{\,s}$ is small because s^4 and s^6 are small (10^{-12} and 10^{-18} for a typical beam with $s = 10^{-3}$). For large partial waves, the $O(s^4)$ and $O(s^6)$ terms contribute significantly. But then $\alpha \approx \beta \approx 1$ with a high accuracy, again validating relation (32). The same argument holds for higher powers of s as well.

Relation (32) implies that we may introduce a modified localized approximation and a modified localization operator,

$$\hat{L}^{\text{mod}} f(R, \theta) = f[(n-1)^{1/2}(n+2)^{1/2}, \pi/2], \quad (36)$$

leading to

$$\overline{g_{n,\text{mod}}} = \exp[-s^2(n-1)(n+2)]. \quad (37)$$

The modified localized approximation may also be written as

$$\overline{g_{n,\text{mod}}} = \exp[-s^2\gamma(n + \tfrac{1}{2})^2], \quad (38)$$

where

$$\gamma = \frac{(n-1)(n+2)}{(n+\tfrac{1}{2})^2}. \quad (39)$$

As is shown in Table 1, this ratio also quickly tends to 1 as n increases. Therefore the localized approximation of Eq. (31) is very close to the modified localized approximation of Eq. (37). For $z_0 \neq 0$, these approxi-

Table 1. Coefficients α, β, and γ of Eqs. (34), (35), and (39), Respectively, as a Function of Partial Wave

Partial Wave	α [Eq. (34)]	β [Eq. (35)]	γ [Eq. (39)]
5	1.166667	1.814815	0.925620
10	1.038462	1.144427	0.979592
50	1.001573	1.005518	0.999118
100	1.000396	1.001388	0.999777
500	1.000016	1.000056	0.999991
1000	1.000004	1.000014	0.999998

mations generalize to

$$\overline{g_n} = \left(1 + 2is\frac{z_0}{w_0}\right)^{-1} \exp(ikz_0) \times \exp\left[\frac{-s^2(n + 1/2)^2}{1 + 2isz_0/w_0}\right], \quad (40)$$

$$\overline{g_{n,\mathrm{mod}}} = \left(1 + 2is\frac{z_0}{w_0}\right)^{-1} \exp(ikz_0) \times \exp\left[\frac{-s^2(n-1)(n+2)}{1 + 2isz_0/w_0}\right]. \quad (41)$$

The results shown in Table 1 indicate that the analytical expressions of the localized and the modified localized approximations bear a strong resemblance to the infinite-series standard-beam BSC's. But Eqs. (31) and (37) are built on the first-order beam, and the standard beams incorporate all the higher-order terms. It is a pleasant surprise that the localized approximation that is built on the first-order beam anticipates these higher-order descriptions and includes them in an approximate way. This will prove to be very useful when the standard-beam BSC's are slowly convergent and is examined in more detail in the Section 3.

3. Numerical Discussion of Localized and Standard BSC's

If we insert the localized and the standard BSC's into the beam partial-wave expansions, we generate the localized and the standard beams, respectively. We could then compare the localized- and the standard-beam profiles. This was done for the beam focal waist plane in Refs. 19 and 27. In this paper, instead, we emphasize the comparison between the individual values of the localized and the standard BSC's.

A. Comparison for $z_0 = 0$ and $s \ll 1$

For the case $z_0 = 0$, we compare the values of the BSC's in Tables 2 and 3 for (1) the localized approximation of Eq. (31), labeled LA; (2) the modified localized approximation of Eq. (37) labeled MLA; and (3) the s-expansion method for the first-, third-, and fifth-order approximations to the standard BSC's of Eqs. (22–24). These are labeled D1, D3, D5, respectively. Also compared are (4) the standard-beam values obtained from Eq. (21) when k is increased until a convergence of 9 significant figures is achieved. The values of k for convergence is listed in Tables 2 and 3, as is the numerical value of g_n^*. The results shown in Table 2 are for the commonly encountered situation of $s = 0.001$.

First we consider the convergence of Eq. (21) for the standard-beam BSC's for $s = 0.001$, which are typical of laser Doppler and phase Doppler instruments,[1–3] and that correspond to focusing of the beam to a radius $w_0 \approx 150\lambda$. The evaluation of g_n^k has been carried out by the use of the symbolic computation software MAPLE. This is compulsory because when one is evaluating the standard coefficients, the number of digits required in the computations to obtain 9 significant figures in the results may be far beyond what is available with FORTRAN double precision variables. MAPLE allows one to carry out evaluations with an arbitrary number of significant figures, which is only limited by the host-computer available storage, by setting the MAPLE variable digits to a prescribed value. For instance, digits = 12 is enough to evaluate g_n^k for small n. For $n = 2500$, the evaluation of g_n^{31} requires digits = 20, and for $n = 5000$, the evaluation of g_n^{101} requires digits = 40. Therefore, although the standard BSC's provide benchmark values for the BSC's that describe a focused Gaussian beam, such benchmark values may in practice be difficult to obtain for large partial waves and tightly confined beams.

Examining the sequence of g_n^k's for various partial waves n and various beam orders k, we may follow the convergence of the standard scheme. Up to the partial wave $n = 5$, g_n^1 is sufficient; i.e., the standard BSC's are correctly evaluated only by the use of first-order Davis beam. For $10 \lesssim n \lesssim 100$, the use of the third-order Davis beam is required. Eventually it is necessary to rely on the kth-order standard scheme with k values larger than 5. For example, for $n = 1000$, 2500, and 5000 we need $k = 15$, 31, and 101, respectively. Large partial waves n are associ-

Table 2. BSC's as a Function of Partial Wave for $s = 0.001$ for the Localized Approximation (LA); the Modified Localized Approximation (MLA); the First- (D1), Third- (D3), and Fifth-order (D5) approximations to the Standard Beam; and the Standard Beam (S)[a]

n	LA	MLA	D1	D3	D5	k, S
1	0.999997750	1.000000000	1.000000000	1.000000000	1.000000000	1, Same as D1
2	0.999993750	0.999996000	0.999996000	0.999996000	0.999996000	1, Same as D1
5	0.999969750	0.999972000	0.999972000	0.999972000	0.999972000	1, Same as D1
10	0.999889756	0.999892006	0.999892000	0.999892006	0.999892006	3, Same as D3
50	0.997452999	0.997455243	0.999452000	0.999455238	0.997455238	3, Same as D3
100	0.989950586	0.989952813	0.080902000	0.989952793	0.989952793	3, Same as D3
1000	0.367511653	0.367512480	<0	0.332834669	0.366292083	15, 0.367511867
2500	0.001925633	0.001925638	<0	<0	<0	31, 0.001925639
5000	0.138186×10^{-10}	0.138187×10^{-10}	<0	<0	<0	101, 0.138208×10^{-10}

[a]For the standard beam, the number of terms in the infinite series of Eq. (27) required for convergence to 9 significant figures (k) is also given.

Table 3. BSC's as a Function of Partial Wave for $s = 0.16$ for the Localized Approximation (LA); the Modified Localized Approximation (MLA); the First- (D1), Third- (D3), and Fifth-Order (D5) Approximations to the Standard Beam; and the Standard Beam (S)[a]

n	LA	MLA	D1	D3	D5	k, S
1	0.944027482	1.000000000	1.000000000	1.000000000	1.000000000	1, Same as D1
2	0.852143789	0.902668412	0.897600000	0.897600000	0.897600000	1, Same as D1
4	0.595472542	0.630778820	0.539200000	0.616138215	0.618138215	3, Same as D3
6	0.339052607	0.359155441	<0	0.327063245	0.343026339	5, Same as D5
10	0.059463060	0.062988600	<0	<0	<0	9, 0.058365667
15	0.002132629	0.002259075	<0	<0	<0	15, 0.002267813
20	0.000021266	0.000022526	<0	<0	<0	19, 0.000031912
25	0.589603×10^{-7}	0.624562×10^{-7}	<0	<0	<0	25, 1.853835×10^{-7}

[a]For the standard beam, the number of terms in the infinite series of Eq. (27) required for convergence to 9 significant figures (k) is also given.

ated through the localized interpretation with geometric light rays that are passing far from the beam axis.[22,23] Therefore the description of the outer parts of the beam requires higher k orders than the description of the central region. This observation must be reconciled with the previously demonstrated fact[18] that a first-order Davis beam satisfies Maxwell's equations up to $O(s^2)$ uniformly over all space. Our results on the convergence of the standard scheme in Table 2 indicate that the situation is more subtle because the coefficients α_k of the various powers of s can make terms such as $\alpha_k s^k$, $k > 2$, significant if α_k is an increasing function of the partial wave n and if n is big enough. Clearly, for the on-axis case, geometric rays associated with large partial waves possess vanishingly small amplitudes that are ineffective in the light-scattering process, so that a poor evaluation of the corresponding BSC's should not be influential. Note, however, that whether a partial wave is effective also depends on the size of the target particle through the Lorenz–Mie partial-wave scattering amplitudes a_n and b_n. In addition, low partial waves are classically associated with backscattering, and large partial waves with side scattering. Thus, when one compares g_n values such as those in Table 2, where $g_1 \approx 1.0$ and $g_{5000} \approx 10^{-11}$, which is vanishingly small in comparison with g_1, we should actually compare the light scattered in different directions. A more refined discussion should then take into consideration scattering diagrams in an actual scattering process.

We now consider the accuracy of the localized approximation and the modified localization approximation BSC's when compared against the benchmark standard-beam BSC's for $s = 0.001$. In Table 2, the comparison between the modified localized approximation and the standard scheme is excellent. Up to the partial wave $n = 100$, the difference between the modified localized approximation and the standard scheme typically does not exceed 1 part in 10^8. Even for $n = 5000$, the disagreement lies in the fifth significant figure. There the modified localized approximation based on the first-order Davis beam anticipates the information contained in the 101st order of the standard scheme. This unexpected internal coherence is considered as a cross-check of the validity of the modified localized approximation, and of the fact that standard beams should be considered as the ideal reference beams. Finally, the localized approximation agrees reasonably well with the standard BSC values. But the agreement for the modified localized approximation is better, especially for $n < 100$.

B. Comparison for $z_0 = 0$ and $s = 0.16$

Table 3 now provides a comparison for $z_0 = 0$ and $s = 0.16$ [i.e., $1/(2\pi)$] near the theoretical confinement limit. The range of important partial waves is much smaller than in Table 2. This is a direct consequence of the localized interpretation; i.e., a BSC of partial wave n is associated with the amplitude of the geometric light ray that is passing at a distance

$$\rho_n = \frac{(n + \frac{1}{2})\lambda}{2\pi} \tag{42}$$

from the beam axis at the focal waist. From relation (32) it can be seen that the amplitude decreases to $1/e^2$ of its value on the z axis for $n \approx 1500$ if $s = 10^{-3}$ and for $n \approx 10$ if $s = 0.16$. The n values are strongly correlated with the necessity of using bigger k orders to obtain convergence for the standard-beam BSC's.

There is also an increase in the difference between the modified localized approximation and the standard values. This difference is dramatic for $n = 25$. There is also an increased difference between the localized and the modified localized approximations. Also, depending on the partial wave n, the modified localized approximation may compare more favorably or less favorably with the standard BSC values than the localized approximation. The deterioration of the comparisons for $s = 0.16$ is consistent with the approach to the physical confinement limit.

C. Comparison for $z_0 \neq 0$

We now focus our attention on the convergence of the standard-beam BSC's for the general on-axis case $z_0 \neq 0$, with $g_n^{\,k}$ given by Eq. (26). Computations are carried out by means of a MAPLE procedure, increasing k in Eq. (25) until the convergence test $g_n^{\,k} = g_n^{\,k-2}$ is satisfied to an accuracy of 50 significant figures.

The value of k for which convergence is reached is denoted by K. In Fig. 2, K is displayed versus z_0 for g_1^s, the BSC for the first partial wave. The beam-waist radius w_0 is used as a parameter. The number of terms required for convergence increases when z_0 increases and when w_0 decreases, i.e., when the focal waist of a tightly focused beam is far upstream or downstream from the origin of coordinates. The increase versus z_0 is particularly sharp for the most focused beam ($w_0 = 0.25$ μm, $s = 0.32$) at the upper limit of the physical confinement range. Figure 3 presents the same data shown in Fig. 2 versus the dimensionless quantity z_0/l, in which l is the spreading length. Because of the fact that l is the natural characteristic length to rescale the z coordinate, all the curves in Fig. 2 collapse to a single curve in Fig. 3.

In Figs. 2 and 3 only the first partial wave was considered. To extend the analysis to all partial waves, K is presented in Fig. 4 as $K(D, z_0/l)$. In Fig. 4 z_0 is still rescaled by l. Rather than the partial wave n, the ordinate is now taken to be

$$D = (n - 1)^{1/2}(n + 2)^{1/2}s, \tag{43}$$

which is the distance ρ from the beam axis associated with n through the modified localized interpretation [Eq. (44), below] and rescaled by w_0. Figure 4, for $\lambda = 0.5$ μm, $w_0 = 5$ μm, and $s = 0.016$, demonstrates how the number of terms required for convergence increases when z_0 or n increases.

To some extent, these results might be considered troubling. Consider, for instance, a small value for s, which leads us to expect that the beam may be safely described by a first-order Davis beam. Figure 4, however, tells us that this conclusion is true only in a small region that surrounds the beam-waist center and that the standard-beam BSC's will be slowly convergent otherwise. Fortunately, as mentioned above, the localized approximation anticipates the behavior of high-order Davis beams and therefore may be used in this case as an alternative to the standard-beam procedure to provide a fast and accurate way to evaluate BSC's. This is the most important result of this paper. When one is computing light scattering with the GLMT formalism, the description of the incident beam should be accurate and should permit scattering calculations to be performed rapidly. The standard-beam BSC's yield the best description of the beam. But in certain circumstances their slow convergence causes a large increase in the computer run time of scattering calculations. The localized approximation, on the other hand, satisfies both criteria of accuracy and computational speed, making it a useful tool in GLMT calculations.

The comparison between the standard, localized, and modified localized BSC's may be complicated in

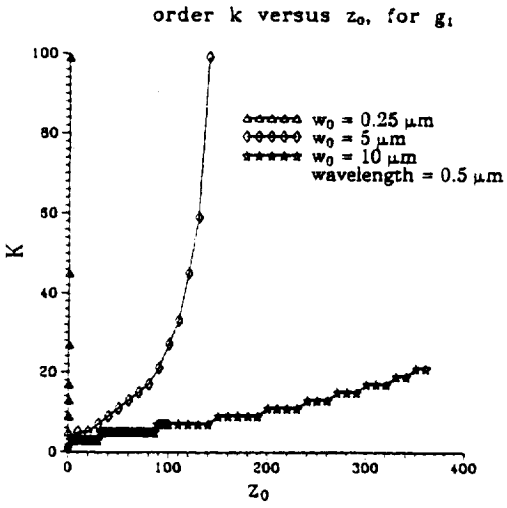

Fig. 2. Value K of the kth-order standard beam required for convergence of the BSC g_1^s as a function of z_0.

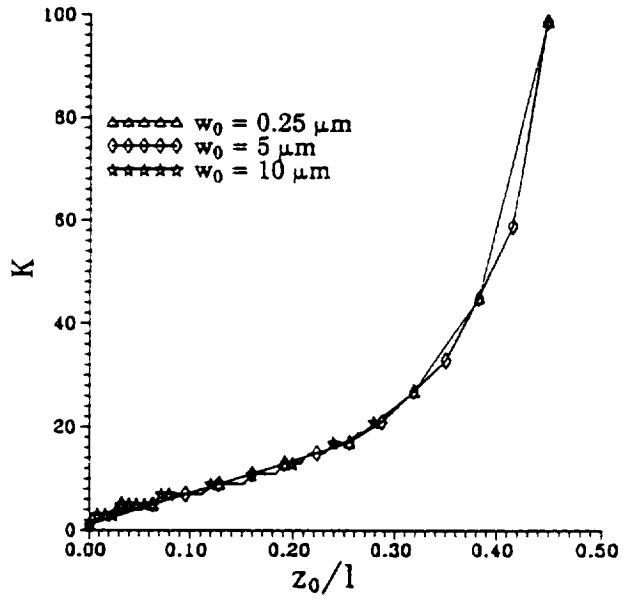

Fig. 3. Value K of the kth-order standard beam required for the convergence of the BSC g_1^s as a function of z_0/l. The individual curves from Fig. 2 now coincide.

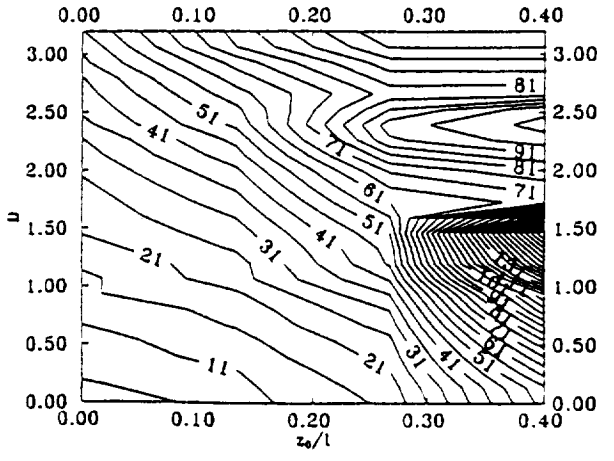

Fig. 4. Value K of the kth-order standard beam required for the convergence of the BSC g_n^s as a function of z_0/l and $D = s(n - 1)^{1.2}(n + 2)^{1.2}$ for $\lambda = 0.5$ μm, $w_0 = 5$ μm, and $s = 0.016$.

the so-called off-axis case, when only one side of the particle is illuminated by the beam. To investigate this problem, it is necessary to design an expansion method for higher-order Davis beams and corresponding off-axis standard-beam expressions. As of yet, this task has not been undertaken, to our knowledge.

4. Top-Hat Beams

Originally, the localized approximation for a focused Gaussian beam was obtained by analogy to van de Hulst's localization principle for plane waves. This led us to associate a BSC g_n with the amplitude of a geometric light ray that is passing at a distance ρ_n from the beam axis, in which ρ_n is given by Eq. (42). In the modified localized approximation, we have

$$\rho_n = (n - 1)^{1/2}(n + 2)^{1/2}\frac{\lambda}{2\pi}. \tag{44}$$

These relations allow us to investigate light scattering by the use of the localized approximation for beams more general than Gaussian beams. For instance, consider top-hat beams, which are used in certain optical particle-sizing instruments.[7–10] Top-hat beam scattering has been calculated previously with the localized approximation, without, however, directly demonstration of the validity of the localized approach to the case of top-hat beams.[10] An assessment of this validity is provided here, illustrating the potentialities of the localized interpretation. We consider an idealized beam profile defined by Eq. (20) in which

$$f(kr, \theta) = \begin{cases} 1 & \text{if } r \sin\theta \le w_0 \\ 0 & \text{if } r \sin\theta > w_0, \end{cases} \tag{45}$$

corresponding to the plateau region of constant illumination of radius w_0 around the beam axis. If we rely on the localized interpretation of Eq. (30), such a beam should be generated by localized BSC's given by

$$\bar{g}_n = \begin{cases} 1 & \text{if } n \le kw_0 - \tfrac{1}{2} \\ 0 & \text{if } n > kw_0 - \tfrac{1}{2} \end{cases}. \tag{46}$$

The accuracy to which Eq. (46) describes a top-hat beam was tested in the following way. It is known that a given set of BSC's g_n defines an on-axis laser beam that is an exact solution of Maxwell's equations. The electric-field components of this beam in the beam-waist plane (i.e., $\theta = \pi/2$) are given by

$$E_x(kr, \pi/2, \phi) = F_1(kr) - F_2(kr)\sin^2\phi, \tag{47}$$

$$E_y(kr, \pi/2, \phi) = F_3(kr)\sin\phi\cos\phi, \tag{48}$$

$$E_z(kr, \pi/2, \phi) = F_3(kr)\cos\phi, \tag{49}$$

with similar relations for the magnetic fields' components. The function F_1 describes the dominant shape of the beam profile, and F_2 and F_3 denote corrections to the dominant shape induced by variations in **E** and **H** in the x–y plane. The explicit forms of the functions F_1, F_2, F_3 in terms of the BSC's are given in Ref. 19.

For the localized beam model of Eq. (46) the dominant shape function $F_1(kr)$ was calculated for the top-hat profile laser beam, for $w_0 = 25$ μm, 7.5 μm, and 2.5 μm, and is shown in Figs. 5(a)–5(c). The results are generally encouraging. The fields are virtually constant from the z axis out to the radius w_0 in the x–y plane as hoped. But beyond w_0, instead of being rigorously zero, the fields are oscillatory, with a slowly decreasing amplitude. This is reminiscent of the oscillatory ringing in the Fourier transform of a function with a hard edge.[29] As the radius of the top-hat beam w_0 decreases, the oscillations become coarser and their amplitude increases. For example, when $w_0 = 25$ μm, the amplitude of the oscillations falls by an order of magnitude from its value in the plateau region when the distance ρ from the z axis is approximately $1.2\,w_0$. For $w_0 = 2.5$ μm this occurs when $\rho \approx 1.7w_0$. The exact effect that these oscillations in the localized electric and magnetic fields have on the far-field scattered intensity calculated in the GLMT framework is not known. But it is expected to be small because the amplitude of the oscillations is only a small fraction of E_0, the field strength in the plateau region.

The sharp cutoff in Eq. (45), however, is not observed in oscilloscope traces of experimental beam profiles.[7] In actuality, the fields possess a smooth but rapid roll-off for $\rho > w_0$. A more realistic model of a top-hat beam is then

$$f(kr, \theta) = \begin{cases} 1 & \text{if } r \sin\theta \le w_0 \\ \exp[-(r \sin\theta - w_0)^2/\epsilon^2] & \text{if } r \sin\theta > w_0, \end{cases} \tag{50}$$

where ϵ is the small roll-off distance of the beam in the x–y plane. The localized beam model for Eq. (50) with the prescription of Eq. (30) is then

$$\bar{g}_n = \begin{cases} 1 & \text{if } n \le kw_0 - \tfrac{1}{2} \\ \exp[-(n + \tfrac{1}{2} - kw_0)^2/k^2\epsilon^2] & \text{if } n > kw_0 - \tfrac{1}{2}. \end{cases} \tag{51}$$

The dominant shape function F_1 of the beam defined by Eq. (51) was calculated for $w_0 = 25$ μm and $\epsilon = 0.05w_0$, and is shown in Fig. 6(a). The oscillations in the field persist for $\rho \ge w_0$. But their amplitude has now been decreased to less than $10^{-3}\,E_0$, and their effect on the far-field scattered intensity is similarly reduced. This decrease is confirmed in Fig. 6(b) for $w_0 = 25$ μm with the more gradual roll-off $\epsilon = 0.1w_0$. The oscillation level has now decreased to less than $10^{-4}E_0$ and is again reminiscent of the reduction in the oscillatory ringing in the Fourier transform of a function with a smooth, gradual edge.[29] The results in this section therefore further support the localized interpretation of partial-wave analyses and provide a

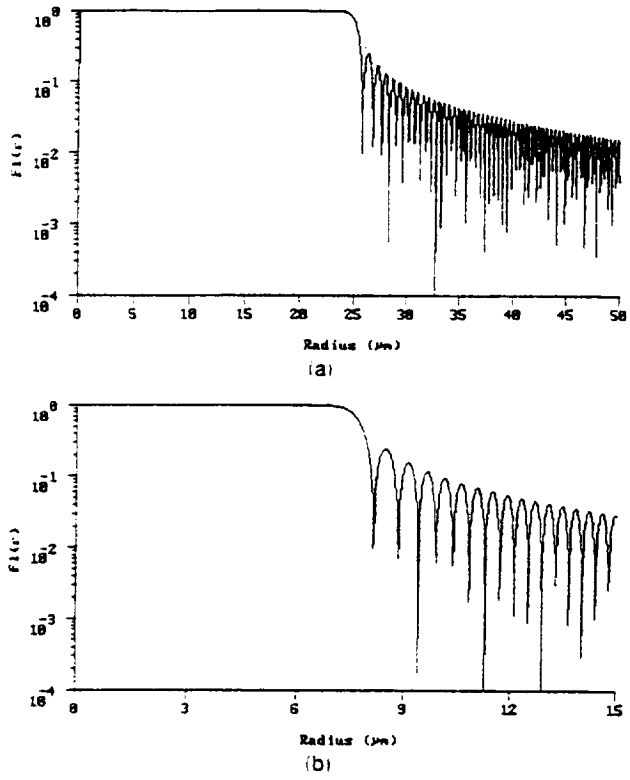

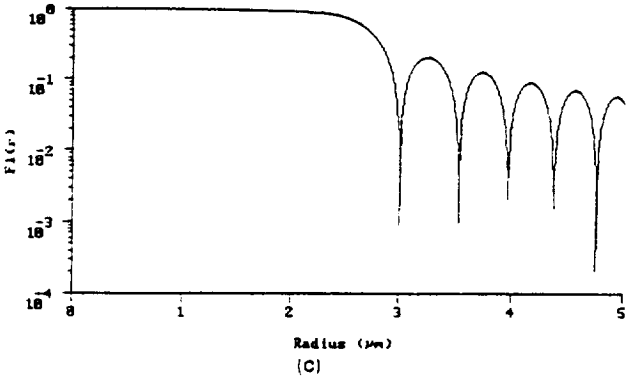

Fig. 5. Dominant beam-shape function F_1 for the localized top-hat beam of Eq. (45) with (a) $w_0 = 25$ μm, (b) $w_0 = 7.5$ μm, and (c) $w_0 = 2.5$ μm as a function of the distance ρ from the z axis.

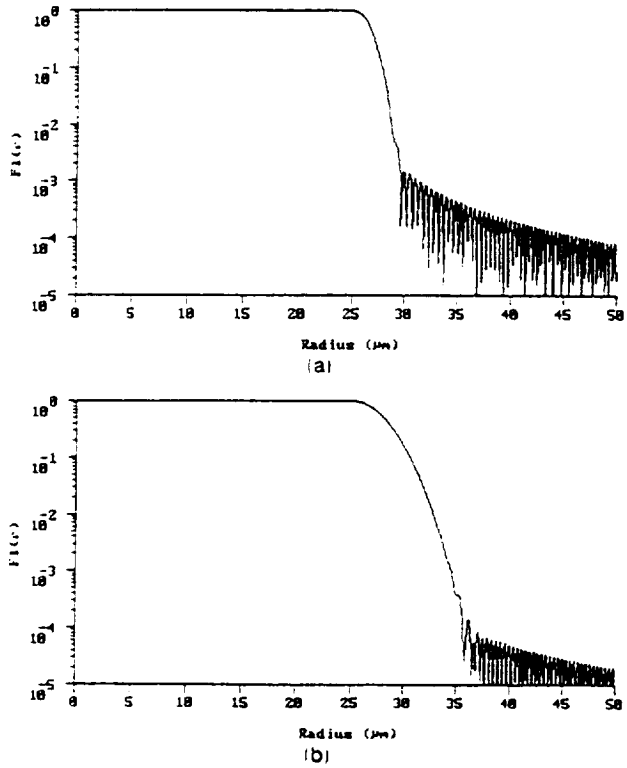

Fig. 6. Dominant beam-shape function F_1 for the localized top-hat beam of Eq. (50), which possesses a smooth roll-off of width ϵ. The curves are for $w_0 = 25$ μm and (a) $\epsilon = 0.05w_0$ and (b) $\epsilon = 0.10w_0$. The smoothing of the edge of the beam profile dramatically decreases the oscillatory ringing in F_1.

new localized description of top-hat beams [eq. (51)], which improves on the description of Eq. (46) previously published in Ref. 10.

5. Conclusion

In the GLMT framework, the question what are the electromagnetic fields of a laser beam is equivalent to the question what are the values of the BSC's that describe the beam? By the use of a so-called *s*-expansion method, one may obtain the fields of standard beams associated with standard BSC's. We claim that these coefficients represent an ideal description of a Gaussian beam. Standard beams make possible the study of both mildly focused and extremely focused beams. The so-called localized approximation received a rigorous justification. It provides a simple analytical expression for the BSC's that is very close to standard beam values. Finally, the localized interpretation of partial-wave expansions that underlies the localized approximation received further support from the investigation of top-hat beams, because they may be accurately described with the localized approximation.

This work was supported in part by National Aeronautics and Space Administration grant NCC-3-204.

References

1. G. Gréhan, G. Gouesbet, A. Naqwi, and F. Durst, "Particle trajectory effects in phase-Doppler systems: computations and experiments," Part. Part. Syst. Charact. **10**, 332–338 (1993).

2. G. Gréhan, G. Gouesbet, A. Naqwi, and F. Durst, "Trajectory ambiguities in phase-Doppler systems: study of a near-forward and a near-backward geometry," Part. Part. Syst. Charact. **11**, 133–144 (1994).
3. S. A. Schaub, D. R. Alexander, and J. P. Barton, "Theoretical analysis of the effects of particle trajectory and structural resonances on the performance of a phase-Doppler particle analyzer," Appl. Opt. **33**, 473–483 (1994).
4. K. F. Ren, G. Gréhan, and G. Gouesbet, "Laser sheet scattering by spherical particles," Part. Part. Syst. Charact. **10**, 146–151 (1993).
5. G. Gréhan, K. F. Ren, G. Gouesbet, A. Naqwi, and F. Durst, "Evaluation of a particle sizing technique based on laser sheets," Part. Part. Syst. Charact. **11**, 101–106 (1994).
6. K. F. Ren, G. Gréhan, and G. Gouesbet, "Evaluation of laser-sheet beam shape coefficients in generalized Lorenz–Mie theory by using a localized approximation," J. Opt. Soc. Am. A **11**, 2072–2079 (1994).
7. D. Allano, G. Gouesbet, G. Gréhan, and D. Lisiecki, "Droplet sizing using a top-hat laser beam technique," J. Phys. D **17**, 43–58 (1984).
8. G. Gréhan and G. Gouesbet, "Simultaneous measurements of velocities and sizes of particles in flows using a combined system incorporating a top-hat beam technique," Appl. Opt. **25**, 3527–3538 (1986).
9. M. Maeda and K. Hishida, "Application of top-hat laser beam to particle sizing in LDV system," in *Proceedings of the First International Symposium on Optical Particle Sizing: Theory and Practice* (Plenum, New York, 1988).
10. F. Corbin, G. Gréhan, and G. Gouesbet, "Top-hat beam technique: improvements and application to bubble measurements," Part. Part. Syst. Charact. **8**, 222–228 (1991).
11. G. Gréhan and G. Gouesbet, "Optical levitation of a single particle to study the theory of the quasi-elastic scattering of light," Appl. Opt. **19**, 2485–2487 (1980)
12. G. Gouesbet, B. Maheu, and G. Gréhan, "Light scattering from a sphere arbitrarily located in a Gaussian beam, using a Bromwich formulation," J. Opt. Soc. Am. A **5**, 1427–1443 (1988).
13. J. P. Barton, D. R. Alexander, and S. A. Schaub, "Internal and near-surface electromagnetic fields for a spherical particle illuminated by a focused laser beam," J. Appl. Phys. **64**, 1632–1639 (1988).
14. G. Gouesbet, G. Gréhan, and B. Maheu, "Generalized Lorenz–Mie theory and applications to optical sizing," in N. Chigier ed., *Combustion Measurements* (Hemisphere, New York, 1991), pp. 339–384.
15. G. Gouesbet, "Generalized Lorenz–Mie theory and applications," Part. Part. Syst. Charact. **11**, 22–34 (1994).
16. L. W. Davis, "Theory of electromagnetic beams," Phys. Rev. A **19**, 1177–1179 (1979).
17. J. P. Barton and D. R. Alexander, "Fifth-order corrected electromagnetic field components for a fundamental Gaussian beam," J. Appl. Phys. **66**, 2800–2802 (1989).
18. G. Gouesbet, B. Maheu, and G. Gréhan, "The order of approximation in a theory of the scattering of a Gaussian beam by a Mie scatter center," J. Opt. (Paris) **16**, 239–247 (1985); republished in *Selected Papers On Light Scattering*, M. Kerker, ed., Vol. 951 of SPIE Milestone Series (Society of Photo-Optical Instrumentation Engineers, Bellingham, Wash., 1988), Part 1, pp. 352–360.
19. J. A. Lock and G. Gouesbet, "Rigorous justification of the localized approximation to the beam-shape coefficients in generalized Lorenz–Mie theory. I: On-axis beams," J. Opt. Soc. Am. A **11**, 2503–2515 (1994).
20. G. Gréhan, B. Maheu, and G. Gouesbet, "Scattering of laser beams by Mie scatter centers: numerical results using a localized approximation," Appl. Opt. **25**, 3539–3548 (1986).
21. J. A. Lock, "Contribution of high-order rainbows to the scattering of a Gaussian laser beam by a spherical particle," J. Opt. Soc. Am. A **10**, 693–706 (1993).
22. B. Maheu, G. Gréhan, and G. Gouesbet, "Ray localization in Gaussian beams," Opt. Commun. **70**, 259–262 (1989).
23. H. C. van de Hulst, *Light Scattering by Small Particles* (Dover, New York, 1981), Sects. 12.31, 12.33.
24. G. Gouesbet, G. Gréhan, and B. Maheu, "Expressions to compute the coefficients g_n^m in the generalized Lorenz–Mie theory, using finite series," J. Opt. (Paris) **19**, 35–48 (1988).
25. G. Gouesbet, G. Gréhan, and B. Maheu, "Computations of the coefficients g_n in the generalized Lorenz–Mie theory using three different methods," Appl. Opt. **27**, 4874–4883 (1988).
26. G. Gouesbet, G. Gréhan, and B. Maheu, "A localized interpretation to compute all the coefficients g_n^m in the generalized Lorenz–Mie theory," J. Opt. Soc. Am. A **7**, 998–1007 (1990).
27. G. Gouesbet and J. A. Lock, "Rigorous justification of the localized approximation to the beam-shape coefficients in generalized Lorenz-Mie theory. II: Off-axis beams," J. Opt. Soc. Am. A **11**, 2516–2525 (1994).
28. S. A. Schaub, J. P. Barton, and D. R. Alexander, "Simplified scattering coefficients for a spherical particle located on the propagation axis of a fifth-order Gaussian beam," Appl. Phys. Lett. **55**, 2709–2711 (1989).
29. G. Arfken, *Mathematical Methods for Physicists*, 3rd ed. (Academic, New York, 1985), Chap. 15.